X-Band Ladder-Line Traveling-Wave Maser*

G. I. HADDAD† AND J. E. ROWE†, SENIOR MEMBER, IRE

Summary—An *X*-band ruby traveling-wave maser (TWM) has been constructed and tested in which the RF structure is a double-ridge ladder line and the signal is coupled into and out of the structure with coaxial lines. The pump power is propagated in a waveguide mode and the device is operated at and below liquid helium temperatures. A four-inch electromagnet was used. The TWM was operated at the push-pull point with a pump frequency of 24 Gc and a signal frequency of approximately 9.65 Gc; the magnetic field was 4.1 kilogauss.

Electronic gains of 15 db have been obtained and bandwidths as high as 130 Mc were observed. Reduced structure losses and longer sections of ruby promise a $G^{1/2}B$ of 1100 Mc (30 db over 35 Mc).

Introduction

THE THEORY and advantages of a traveling-wave maser have been given in the literature[1-3] and various means of slowing the velocity of the propagating wave have been discussed. The highest frequency traveling-wave maser that was known to the authors at the inception of this work was that of De Grasse, *et al.*,[1] of the Bell Telephone Laboratories. This maser had an operating frequency around 6 kMc. The extension of the traveling-wave maser to higher frequencies was the main objective of this work. The Karp-type slow-wave structure[4] was chosen and experiments to evaluate the possibilities of this structure as a traveling-wave maser circuit at higher frequencies have been performed. These investigations were carried out in the *X*-band frequency range; extension to higher frequencies is a matter of scaling the dimensions to the proper frequency range.

A few words justifying the choice of the Karp structure are in order here. The characteristics of the Karp structure are very similar to those of the Comb structure[1] since both are of the resonant slowing type and have a definite pass band with associated upper and lower cutoff frequencies. However, since in the Karp structure the fingers are rigidly supported on both sides while in the Comb structure they are only supported on one side, the former gives a more rugged mechanical structure, especially at higher frequencies where the dimensions of the fingers become minute.

* Received by the PGMTT, May 19, 1961; revised manuscript received, August 8, 1961. This work was supported by Project MICHIGAN under Contract No. DA 36-039 sc-78801.

† Electron Physics Laboratory, Department of Electronic Engineering, The University of Michigan, Ann Arbor, Mich.

[1] R. W. De Grasse, *et al.*, "The three-level solid state traveling-wave maser," *Bell Sys. Tech. J.*, vol. 38, pp. 305–335; March, 1959.

[2] W. S. C. Chang, *et al.*, "Cavity and traveling-wave masers using ruby at S-band," 1959 IRE WESCON CONVENTION RECORD, pt. 1, pp. 142–150.

[3] H. D. Tenney, *et al.*, "An *S*-band traveling-wave maser," 1959 IRE WESCON CONVENTION RECORD, pt. 1, pp. 151–155.

[4] A. Karp, "Traveling-wave tube experiments at millimeter wavelengths with a new, easily built, space harmonic circuit," PROC. IRE, vol. 43, pp. 41–46; January, 1955.

Karp-Type Slow-Wave Structure

The Karp-type structure possesses all of the characteristics[1] which are essential in a traveling-wave maser application. Very high slowing factors can be obtained by adjusting the dimensions and by properly loading the structure with a dielectric which in this case can be the active maser material itself. The RF magnetic field has different senses of circular polarization above and below the plane of the fingers and, therefore, unilateral gain and attenuation can be obtained by placing the active maser material below the fingers and the isolation material above the fingers. The magnetic field intensity is maximum at the shorted ends of the fingers and zero in the middle. The electric field is maximum in the middle of the fingers and zero at the shorted ends. Thus, by placing a dielectric material such as ruby next to the side walls, effective magnetic coupling can be achieved without producing high dielectric loading, which might otherwise affect the structure characteristics considerably.

The microwave pump power, which is necessary to invert the spin population in the paramagnetic crystal, can be propagated in the ridged waveguide which encloses the ladder line. If this power propagates through the waveguide in a TE_{10} mode, and the ladder line is placed in the middle of the waveguide, a minimum amount of coupling between the waveguide mode and the ladder will result. The waveguide can be shorted at one end and a coupling iris placed at the other end to enhance the coupling of the pumping field to the maser crystal.

The group velocity, which is needed to compute the gain, and the tunable bandwidth of the maser can be computed from the frequency vs phase shift per section characteristics of the slow-wave structure. Since these characteristics are essentially the same in the double- and single-ridge Karp structures, the phase vs frequency characteristics of the single-ridge structure have been analyzed in detail. The effect of dielectric materials placed in different regions of the structure, namely, in the middle and at the sides, has also been considered.

Fig. 1 shows a single-ridge Karp structure. The material on the sides has a relative dielectric constant ϵ_{r1}, which in this case is that of the active maser material, ruby, whose $\epsilon_r = 9$. The material between the ridge and the ladder has a relative dielectric constant ϵ_{r2}. This material can be either rutile ($\epsilon_r \approx 100$) or air ($\epsilon_r = 1$).

In order to predict the phase vs frequency characteristics, the structure is replaced by an equivalent circuit which is shown in Fig. 2. The fingers are considered as two shorted transmission lines with a characteristic im-

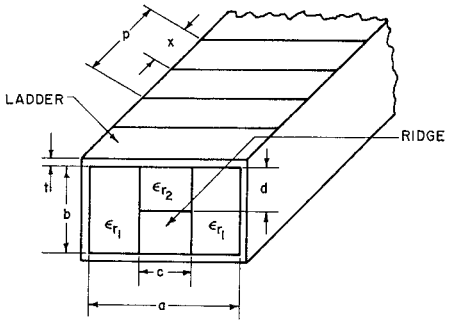

Fig. 1—TWM structure.

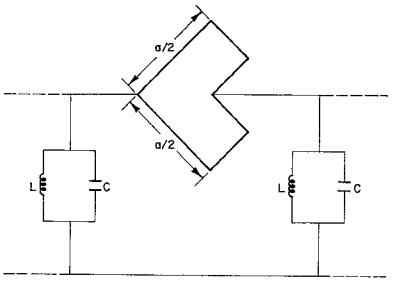

Fig. 2—Karp structure equivalent circuit.

pedance of Z_0. L and C include the effect of the ridge and the dielectric material. The equivalent circuit representation does not take into account the coupling between slots; however, the results obtained from this approximate representation agree quite well with the experimental results. They also agree qualitatively with Butcher's[5] results, where the ladder is approximated by a uniform sheet which conducts only in the direction of the ladder and an exact solution is obtained.

For the equivalent circuit of Fig. 2 the lower frequency cutoff occurs when the admittance of the shunt arm is equal to zero. This can be expressed as

$$Y_{\text{shunt}} = \frac{1}{j2\pi f_c L} + j2\pi f_c C = 0, \tag{1}$$

where f_c is the lower cutoff frequency. L is then expressed as

$$L = \frac{1}{\omega_c^2 C}, \tag{2}$$

where $\omega_c = 2\pi f_c$. The susceptance of the shunt arm is conveniently written as

$$B_{\text{shunt}} = j\omega C\left[1 - \left(\frac{\omega_c}{\omega}\right)^2\right]. \tag{3}$$

If the series arm in Fig. 2 is considered as two shorted transmission lines in parallel, the susceptance of this arm, B_{series}, becomes

$$B_{\text{series}} = -j2Y_0 \cot\frac{\beta a}{2}, \tag{4}$$

where

a = the finger length,
Y_0 = the characteristic admittance of the fingers considered as a transmission line, and
β = phase shift in radians per unit length.

If f_1 is taken as the frequency at which the slot length a is one half a free-space wavelength, then (4) becomes

$$B_{\text{series}} = -j2Y_0 \cot\left(\frac{\pi}{2}\frac{f}{f_1}\right). \tag{5}$$

Filter theory is used to relate the phase shift per section θ to the admittances of the series and shunt arms through the following expression:

$$\cos\theta = 1 + \frac{B_{\text{shunt}}}{2B_{\text{series}}}. \tag{6}$$

Substituting the values of B_{shunt} and B_{series} from (3) and (5) into (6) yields

$$\cos\theta = 1 - 2\pi f\left(\frac{CZ_0}{4}\right)\cdot\left[1 - \left(\frac{f_c}{f}\right)^2\right]\tan\left(\frac{\pi}{2}\frac{f}{f_1}\right). \tag{7}$$

Thus, for a certain f_c, f_1 and CZ_0 a phase shift vs frequency curve can be obtained.

The lower cutoff frequency is determined by the waveguide dimensions, the type of dielectric material that is employed, and the location of this material in the waveguide. The cutoff conditions in a ridged waveguide have been presented in the literature.[6,7] The cutoff conditions for a dielectric loaded waveguide, which are of interest here, have also been plotted in Figs. 3 and 4. These graphs enable one to obtain the lower cutoff frequency of the structure and also the cutoff frequency of the TE_{20} mode, which is of interest when the pump power is propagated through the structure in a waveguide mode.

The frequency f_1 is fixed by choice of the length of the fingers. This choice and the amount of capacitive loading that is introduced by the ridge and the dielectric determine the upper cutoff frequency of the slow-wave structure.

The amount of capacitive loading is measured by C, the capacitance of the shunt arm, and can be approximately expressed in terms of the dimensions and the dielectric constant through the expression

$$C \approx \frac{\epsilon c(p - x)}{d}, \tag{8}$$

[5] P. N. Butcher, "A theoretical study of propagation along tape ladder lines," *Proc. IEE*, vol. 104, pt. B, pp. 169–176; March, 1957.

[6] N. Marcuvitz, "Waveguide Handbook," M.I.T. Rad. Lab. Ser., vol. 10, McGraw-Hill Book Co., Inc., New York, N. Y., p. 400; 1951.

[7] S. Hopfer, "The design of ridged waveguides," IRE TRANS. ON MICROWAVE THEORY AND TECHNIQUES, vol. MTT-3, pp. 20–29; October, 1955.

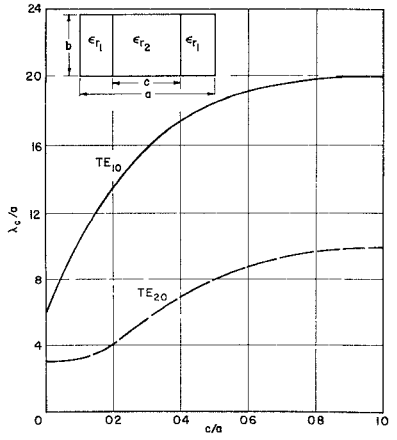

Fig. 3—Cutoff conditions for a dielectric loaded waveguide ($\epsilon_{r_1}=9$, $\epsilon_{r_2}=100$).

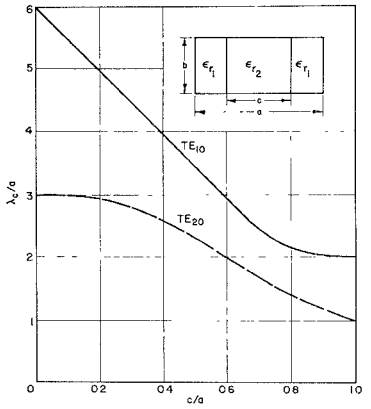

Fig. 4—Cutoff conditions for a dielectric loaded waveguide ($\epsilon_{r_1}=9$, $\epsilon_{r_2}=1$).

where

p = the pitch of the ladder line,
d = the distance between the ridge and the ladder,
c = the width of the ridge,
x = the width of the slot in the ladder, and
ϵ = the dielectric constant of the material between the ridge and the ladder.

The above equation gives an approximate expression for C. The major contribution to C arises from loading at the middle because the electric field is maximum there and becomes zero at the side walls. This value will be increased, however, when a dielectric material is placed on both sides of the ridge as is done in a traveling-wave maser. The increase depends on the extent of the material from the side walls to the ridge and also the extent of the material from the ladder line to the bottom plate.

From transmission line theory, the characteristic impedance Z_0 of (7) can be approximately expressed as

$$Z_0 \approx 120 \ln \frac{x}{t}, \tag{9}$$

where t = the thickness of the ladder line. Thus, CZ_0, which appears in (7), can be written as

$$CZ_0 = \frac{120\epsilon c p}{d}\left(1 - \frac{x}{p}\right) \ln \frac{x}{t}. \tag{10}$$

Thus, for a certain set of dimensions of the structure, f_c, f_1 and CZ_0 can be calculated and (7) can be used to calculate a phase shift vs frequency curve. From this plot the group velocity can be calculated at any frequency in the pass band. Several of these curves have been plotted and are presented in Figs. 5–7.

Phase Shift vs Frequency for the Karp Structure

Fig. 5 illustrates the effect of CZ_0 on the characteristics of the structure. It can be seen from these curves that for a certain lower cutoff frequency f_c and a certain f_1, the upper cutoff frequency is decreased when CZ_0 is increased. This decreases the structure pass band and higher slowing factors result. CZ_0 is related to the structure dimensions and the dielectric constant of the material through (10).

It is obvious from this relation that CZ_0 can be increased in several ways. One way is to decrease d, the distance between the ladder and the ridge. This, however, has a slightly negative effect in that the lower cutoff frequency is decreased when d is decreased while the other dimensions are kept the same. The net effect is favorable, however, because the upper cutoff frequency decreases more rapidly than the lower one and the pass band becomes narrower.

Another way is to increase the dielectric constant of the material between the ridge and the ladder. This has the same effect as decreasing d. The group velocity v_g which can be easily derived from (7), is expressed as follows:

$$\frac{v_g}{p} = \frac{\left\{2\pi f\left[\frac{8}{CZ_0} - 2\pi f\left(1 - \left(\frac{f_c}{f}\right)^2\right)\tan\frac{\pi f}{2f_1}\right]\right\}^{1/2}}{\left\{\left[1 - \left(\frac{f_c}{f}\right)^2\right]\tan\frac{\pi f}{2f_1}\right\}^{1/2}\left[\frac{1 + \left(\frac{f_c}{f}\right)^2}{1 - \left(\frac{f_c}{f}\right)^2} + \frac{\frac{\pi f}{f_1}}{\sin\frac{\pi f}{f_1}}\right]}. \tag{11}$$

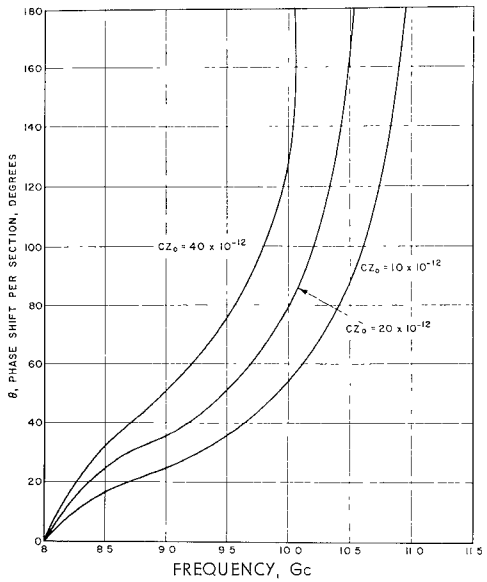

Fig. 5—Phase shift per section, θ, vs frequency with CZ_0 as a parameter ($f_c = 8$ Gc, $f_1 = 11$ Gc).

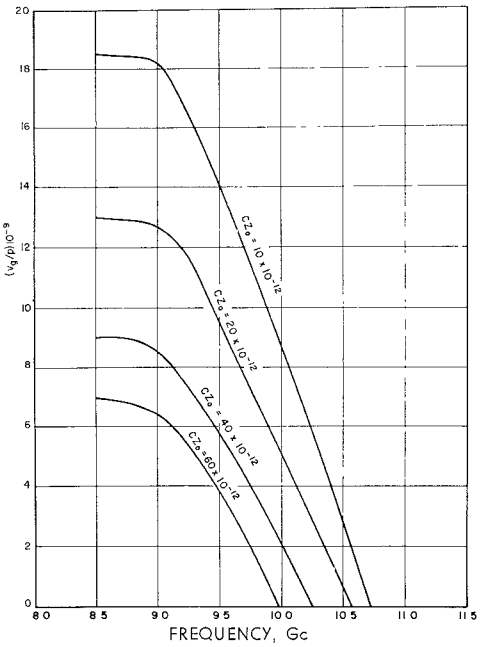

Fig. 6—v_g/p vs frequency for different values of CZ_0. p is the pitch ($f_c = 8$ Gc, $f_1 = 11$Gc).

Graphs of v_g/p vs frequency for different values of CZ_0 and specified values of f_c and f_1 are shown in Fig. 6. These plots show that v_g can be made as small as desirable either by decreasing p or by increasing CZ_0 while keeping f_c fixed. There are limits, however, on how small the pitch can be made. This is due to the fact that as the pitch decreases the fields become more tightly coupled to the fingers, thus decreasing the amount of maser material that can effectively interact with the RF fields. CZ_0 can be increased by increasing the ratio x/t without affecting the lower cutoff frequency.

It has been found that the pass band can be narrowed and higher slowing factors can be obtained by properly loading the structure with a dielectric material. This is illustrated in Fig. 7, where the characteristic of an unloaded structure is compared with that of a ruby-loaded one as shown. For the unloaded structure the lower and upper cutoff frequencies were measured and found to be 8.5 and 12.5 Gc ,respectively. The loaded one showed a lower cutoff frequency of 7.5 Gc and an upper cutoff frequency of 10 Gc. This structure was employed in the traveling-wave maser experiments. Detailed discussion of the traveling-wave maser assembly, the double-ridge Karp structure that was used, and the experimental results are given in the following sections.

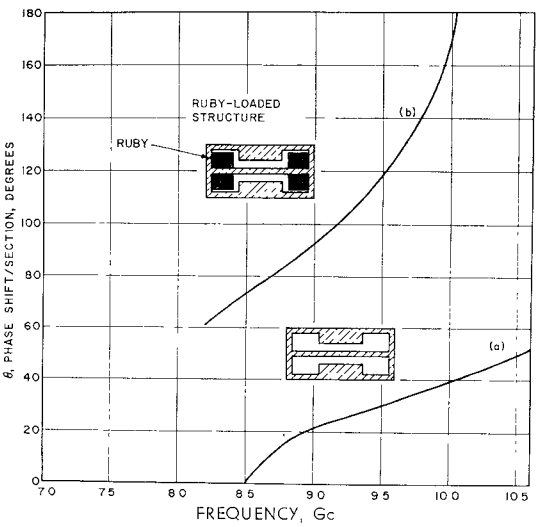

Fig. 7—Phase shift per section θ vs frequency for the double-ridge Karp structure.

Traveling-Wave Maser Assembly

A double-ridge Karp-type slow-wave structure was employed in the traveling-wave maser experiments. The ladder line of this structure has an over-all length of 4 inches, but the effective length of the interaction region was slightly less than 4 inches because the diameter of the pole pieces of the magnet used is only 4 inches. The ladder line was photo-etched and made out of copper. It has a pitch of 0.040 inch, a separation between fingers of 0.020 inch, and a finger length of 0.44 inch. The phase shift vs frequency characteristics of this structure are given in Fig. 7.

The active material that has been used is light ruby, which has approximately 0.05 per cent Cr^{+++} concentration. Both dark ruby, which has approximately 1 per cent Cr^{+++} concentration, and polycrystalline yttrium iron garnet have been used for isolation.

A closeup of the interaction region is shown in the disassembled view of Fig. 8. The coupling of the signal power into and out of the structure is clearly demonstrated in this figure. The outer conductors of the coaxial lines are terminated at one sidewall of the struc-

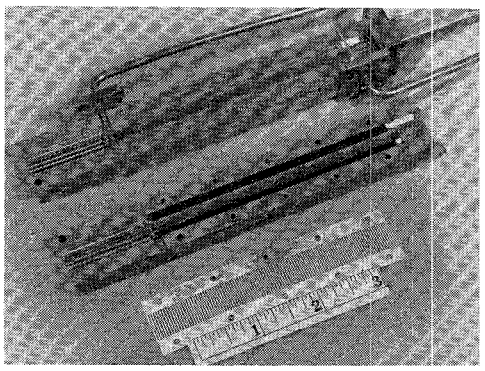

Fig. 8—View of the disassembled traveling-wave maser, showing the ladder line and the location of the ruby crystals.

ture, while the center conductors extend to the other sidewall. These portions of the center conductors are flattened out to the desired thickness and located in the plane of the ladder.

The location of the ruby crystals is also shown in the above figure. Two slabs (each 2 inches long) of light ruby, which is the active material, are placed on each side of the ridge of the bottom plate. These slabs extend all the way along the 4-inch ladder line and are located so that they touch the fingers. The four slabs of dark ruby which provide the isolation are similarly located in the top plate and do not touch the fingers but are very close to them. In recent experiments, however, the dark ruby slabs have been replaced by light ruby and a slab of polycrystalline yttrium iron garnet was placed beside the ruby pieces in the top plate to provide the necessary isolation. A *k*-band waveguide is connected to the structure on one end and the pump power propagates through the structure in a ridged-waveguide mode. The other end of the structure is terminated by an adjustable sliding short.

Experimental Results

With the coupling scheme described in the previous section, standing-wave ratios of 1.5–2.0 were obtained over quite a wide frequency range. The VSWR was found to vary quite abruptly over the pass band of the structure, but adequate matching was obtained at the desired signal frequencies by adjusting the thickness of the flattened portion of the center conductor and its relative position with respect to the ladder line. The appearance of the pass band was improved when an isolating material was incorporated into the structure to suppress the internal resonances in the structure.

The point on the energy level diagram that has been employed in these experiments is the push-pull point.[8,9] This point occurs when the angle between the dc magnetic field and the ruby *c* axis is approximately 55°. At this point of operation and for a pump frequency of approximately 24 Gc, the corresponding signal frequency is around 9.65 Gc and the magnetic field is near 4.1 kilogauss. The *c* axes of the ruby crystals are perpendicular to the plane of the ladder. No other orientation of the *c* axes with respect to the RF fields was investigated.

The insertion loss in the neighborhood of the signal frequency is approximately 10 db at room temperature. At liquid helium temperatures this loss decreased to 5 db. The loss includes the input and output coaxial lines, which have an attenuation of approximately 0.4 db per foot at room temperature. A total of approximately 7 feet of coaxial line was used. The insertion loss can be made lower by using waveguides instead of coaxial cables to couple the signal power into and out of the structure. This, however, makes the maser assembly quite bulky. The loss in the structure can be decreased by an improved assembly. Since the magnetic fields are strongest at the side walls where the top and bottom plates are fastened together, a very good contact at these points will minimize the losses. The screws might not provide a good contact, which would result in higher losses.

When four slabs of dark ruby (two slabs placed on each side of the ridge of the top plate as shown in Fig. 8) were employed for isolation, an absorption of 16–17 db was obtained with the dc magnetic field in the reverse direction and an absorption of approximately 2 db was obtained with the field in the normal direction. These values were obtained at a bath temperature of 4.2°K. Even though the dark ruby material provides good isolation, it was found difficult to align the *c* axes of the several ruby crystals in order to obtain amplification from the light ruby and absorption from the dark ruby at the same value of magnetic field. The dark ruby also absorbs an appreciable amount of pump power, which renders its application as the isolating material less attractive.

In recent experiments on the traveling-wave maser the dark ruby pieces in the top plate were replaced by light ruby pieces. A slab of yttrium iron garnet, cut to the proper size for ferromagnetic resonance and placed beside the light ruby pieces on one side of the ridge in the top plate, was employed for isolation. A forepump was employed to pump the liquid helium in order to reduce its temperature. It was observed that the electronic gain was 2.5 times higher with the forepump on than with it off. The Dewar design did not include a provision for measuring the absolute value of the temperature.

A high degree of nonreciprocity was achieved by using the garnet slab. When the structure was operated simply as an isolator, the ratio of the absorption in db in the backward direction to that in the forward direction was approximately 15. The addition of the garnet slab greatly improved the pass band of the structure. The garnet slab was approximately 0.02 inch×0.09 inch in

[8] W. S. Chang and A. E. Siegman, "Characteristics of ruby for maser applications," Electron Devices Lab., Stanford University, Stanford, Calif., Tech. Rept. No. 156-2; September 30, 1958.

[9] C. Kikuchi, *et al.*, "Ruby as a maser material," *J. Appl. Phys.*, vol. 30, pp. 1061–1067; July, 1959.

cross section and 4 inches long. The loss due to the garnet slab was approximately 30 db in the reverse direction.

When the maser was operated with no isolation, a high degree of regeneration was observed and very large amounts of regenerative gain and oscillations were observed. The bandwidth, on the other hand, decreased sharply. When sufficient isolation was incorporated in the structure, electronic gains of 15 db over a bandwidth of 75 Mc were obtained. The square-root gain bandwidth was 420 Mc.

This amount of gain was obtained, however, at two slightly different signal frequencies by changing the magnetic field while holding the pump frequency fixed. Also at a particular signal frequency, electronic gains of approximately 15 db over a 75-Mc bandwidth were obtained at two slightly different values of dc magnetic field and two corresponding values of pump frequency. This is attributed to the misalignment of the c axes of the several light ruby slabs that have been employed.

In one of the experiments that have been performed, the c axes of the ruby slabs were close enough together to result in electronic gains of approximately 13 db over 130-Mc bandwidth. The total loss in the structure including the isolator was approximately 7 db, which left a net gain of 6 db over 130 Mc.

It is important to note here that the bandwidth over which interaction was obtained was quite high compared to the 3-db bandwidth. This is attributed to the inhomogeneity of the dc magnetic field between the pole pieces, which tends to broaden the line width of the ruby slabs and thus lower the gain. The spacing between the pole pieces was 4 inches, and for this spacing the magnetic field falls off to about 10 per cent of its central value at a radial distance of approximately 1.5 inches.

It can be deduced from the above results that if the c axes of all the ruby slabs were well aligned and the dc magnetic field made more homogeneous, electronic gains of approximately 30 db over a bandwidth of possibly 35–40 Mc could have been obtained. This would correspond to a net gain of approximately 25 db over the same bandwidth, which would correspond to a net gain-bandwidth product of over 700. It is, of course, preferable to use 4-inch ruby slabs in order to minimize the alignment problem. The amplification can be tuned over a frequency range of 9.45 to 9.85 Gc (400 Mc) by adjusting the pump frequency and the magnetic field with a corresponding change in the electronic gain of ∓ 2 db. This change in gain is attributed to the variation of the group velocity in the pass band.

A typical output of the traveling-wave maser showing the electronic gain is presented in Fig. 9, where the bottom trace is the output with no dc magnetic field and the top trace is the output with the dc magnetic field adjusted to resonance and pump power turned on.

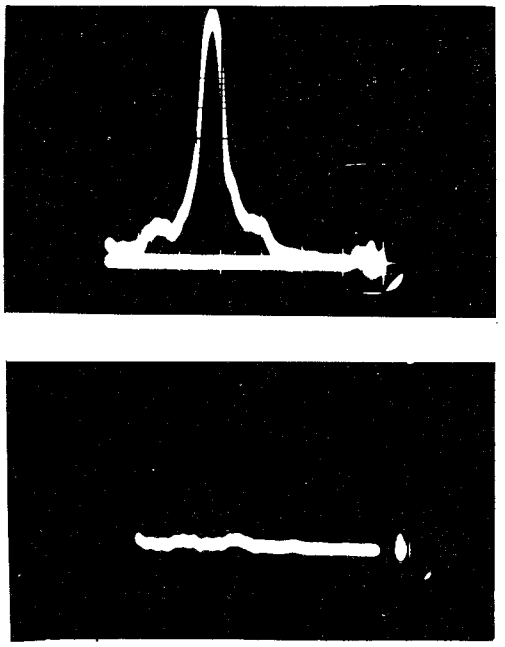

Fig. 9—Electronic gain in the TWM.

Conclusions

It can be concluded that operation of a traveling-wave maser at X band utilizing a Karp-type slow-wave structure is feasible. Electronic gains of 30 db over a 35-Mc ($G^{1/2} \approx 1100$) bandwidth can be obtained at the push-pull point of operation. Even broader bandwidths can be achieved by stagger-tuning either the magnetic field or the ruby crystals as has been demonstrated. The major difficulty has been the alignment of the c axes of the several ruby slabs, which can certainly be overcome through better alignment or by using 4-inch long slabs of ruby. The use of either dark ruby or polycrystalline yttrium iron garnet as the isolating material has been demonstrated and both were found feasible.

Electronic rather than net gain has been emphasized in the measurements because this gives a better measure of the effectiveness of the slow-wave structure as a wave-slowing device. The circuit losses can be improved by fabrication and assembly techniques.

The application of a Karp-type slow-wave structure as a traveling-wave maser circuit can be easily extended into the millimeter wave range. In this range, a very small length of the structure would be required to obtain adequate gain.